

This is a repository copy of *Subtle Microwave-Induced Overheating Effects in an Industrial Demethylation Reaction and Their Direct Use in the Development of an Innovative Microwave Reactor*.

White Rose Research Online URL for this paper:

<https://eprints.whiterose.ac.uk/115748/>

Version: Accepted Version

Article:

De Bruyn, Mario orcid.org/0000-0002-9687-1606, Budarin, Vitaliy L., Sturm, Guido S.J. et al. (4 more authors) (2017) Subtle Microwave-Induced Overheating Effects in an Industrial Demethylation Reaction and Their Direct Use in the Development of an Innovative Microwave Reactor. *Journal of the American Chemical Society*. pp. 5431-5436. ISSN 1520-5126

<https://doi.org/10.1021/jacs.7b00689>

Reuse

Items deposited in White Rose Research Online are protected by copyright, with all rights reserved unless indicated otherwise. They may be downloaded and/or printed for private study, or other acts as permitted by national copyright laws. The publisher or other rights holders may allow further reproduction and re-use of the full text version. This is indicated by the licence information on the White Rose Research Online record for the item.

Takedown

If you consider content in White Rose Research Online to be in breach of UK law, please notify us by emailing eprints@whiterose.ac.uk including the URL of the record and the reason for the withdrawal request.

1 Subtle Microwave-Induced Overheating Effects in an Industrial 2 Demethylation Reaction and Their Direct Use in the Development of 3 an Innovative Microwave Reactor

4 Mario De bruyn,[†] Vitaliy L. Budarin,[†] Guido S. J. Sturm,^{||} Georgios D. Stefanidis,[‡] Marilena Radoiu,[§]
5 Andrzej Stankiewicz,^{||} and Duncan J. Macquarrie^{*,†,||}

6 [†]Green Chemistry Centre of Excellence, University of York, YO10 5DD, Heslington, York, United Kingdom

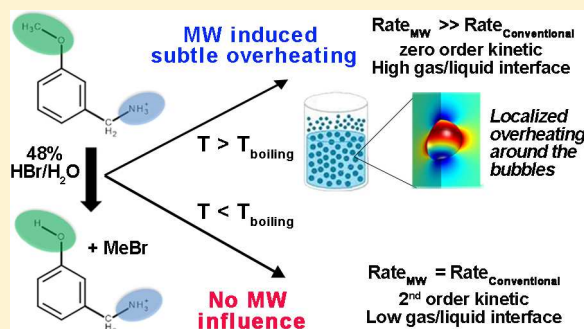
7 [‡]Catholic University of Leuven (KU Leuven), Process Engineering for Sustainable Systems Section, Willem de Croylaan 46-box 2423,
8 3001 Leuven, Belgium

9 [§]SAIREM, 12 Porte du Grand Lyon, 01702 NEYRON Cedex, France

10 ^{||}Process & Energy Department, Delft University of Technology, Leeghwaterstraat 39, 2628CB Delft, The Netherlands

11 **S** Supporting Information

12 **ABSTRACT:** A systematic study of the conventional and microwave
13 (MW) kinetics of an industrially relevant demethylation reaction is
14 presented. In using industrially relevant reaction conditions the
15 dominant influence of the solvent on the MW energy dissipation is
16 avoided. Below the boiling point, the effect of MWs on the activation
17 energy E_a and k_0 is found nonexistent. Interestingly, under reflux
18 conditions, the microwave-heated (MWH) reaction displays very
19 pronounced zero-order kinetics, displaying a much higher reaction
20 rate than observed for the conventionally thermal-heated (CTH)
21 reaction. This is related to a different gas product (methyl bromide,
22 MeBr) removal mechanism, changing from classic nucleation into
23 gaseous bubbles to a facilitated removal through escaping gases/
24 vapors. Additionally, the use of MWs compensates better for the strong heat losses in this reaction, associated with the boiling of
25 HBr/water and the loss of MeBr, than under CTH. Through modeling, MWH was shown to occur inhomogeneously around
26 gas/liquid interfaces, resulting in localized overheating in the very near vicinity of the bubbles, overall increasing the average
27 heating rate in the bubble vicinity vis-à-vis the bulk of the liquid. Based on these observations and findings, a novel continuous
28 reactor concept is proposed in which the escaping MeBr and the generated HBr/water vapors are the main driving forces for
29 circulation. This reactor concept is generic in that it offers a viable and low cost option for the use of very strong acids and the
30 managed removal/quenching of gaseous byproducts.



31 ■ INTRODUCTION

32 The 20th century has been mainly dominated by the use of
33 conventional thermal energy to drive chemical reactions. The
34 use of alternative energy sources, such as microwave (MW)
35 technology, appeared in the late 1970s, and its use could
36 overcome existing bottlenecks in chemical manufacturing and
37 improve the carbon footprint of many reactions.¹ While it is
38 clear that poor instrumentation has led to erroneous reports
39 and set off unrealistic expectations,² a systematic and controlled
40 investigation of the influence of MWs on chemical reactions
41 and their kinetics has been lacking. Such background
42 information is however indispensable for possible future
43 implementation of MW technology on an industrial scale. To
44 date, many types of thermal and nonthermal MW effects have
45 been reported; as a guide to past research in these reports, the
46 interested reader is referred to the critical review by De La Hoz
47 and co-workers.³ Presently, many of the “nonthermal MW
48 effects” have been disproven as being the result of an incorrect

temperature measurement. Also, the energy contained in MWs
49 is far too low to break even hydrogen bonds.⁴ In the presence
50 though of non-MW absorbing solvents the groups of Dudley
51 and Stiegman argue that both substrate and product can
52 temporarily store energy, leading to localized temperature
53 increases at the reactive site, accounting for the observed MW
54 rate enhancements.⁵ More recently they also showed that
55 poorly MW-absorbing molecules can be selectively heated by
56 MWs provided association to a nonreactive polar molecule as a
57 good MW absorber, albeit the effect is then less pronounced.⁶
58 In a further advancement the Kappe group used Si–C vessels
59 which were proclaimed to impede the penetration of MWs into
60 the reaction vessel, heating the Si–C material instead, and thus
61 administering in essence conventional heating. That way no
62 difference in reactivity could be observed between conventional
63

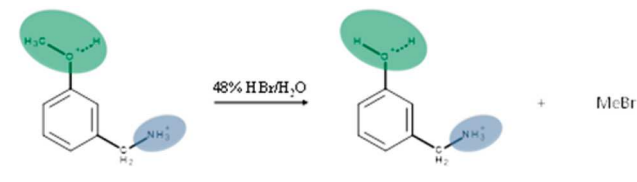
Received: January 26, 2017

Published: March 27, 2017

64 and MW heated reactions.⁷ However, very recently the Strouse
65 group showed convincingly that 3 mm Si–C tube walls only
66 retain ~48% of the MWs, pointing at significant MW
67 transmission into, and dissipation inside, the reaction vessel.

68 This MW leakage through Si–C tube walls is particularly
69 acute when a strongly absorbing solvent is used.⁸ Fan et al. have
70 pioneered the use of MW technology to the hydrothermal
71 depolymerization of cellulose to glucose, demonstrating a
72 distinct influence of the applied MW density and a MW heat
73 input via molecular radiators;⁹ notably, they used proton/
74 deuterium exchange techniques to also obtain structural
75 information. Many research groups continue to propose
76 differing activation energies for reactions run in the presence
77 of CTH vis-à-vis MWH. However, the determination of the
78 kinetic parameters (E_a , k_0) of a reaction strongly depends on
79 the applied model and thus requires a solid understanding of
80 the reaction mechanism. Also, a sufficient number of data
81 points is needed to ensure confidence, thus requiring a
82 thorough analytical method. In this study we have investigated
83 the MW activation of an industrially (pharmaceutically)
84 relevant demethylation reaction, converting (3-
85 methoxyphenyl)methylammonium bromide (3MPMA) into
86 (3-hydroxyphenyl)methylammonium bromide (3HPMA) (see
87 Scheme 1)^{10,11} with a detailed kinetics study. For this purpose,

Scheme 1. Overview of the Reaction



88 we have used both a SAIREM MiniFlow200SS¹² with TM
89 monomode cavity and an Anton Paar Monowave 300, both of
90 which are equipped with fiber-optic temperature measurement.
91 The MiniFlow200 uses a solid-state MW generator, which
92 enables precise frequency and microwave power control; in
93 addition, it features forward and reflected power measurement
94 so that an energy balance can be obtained. The absence of this
95 latter feature in most commonly used MW heating equipment
96 has been demonstrated to result in significant misreadings of
97 the actual MW power transferred to the sample under
98 investigation.¹³ The experimental study is complemented by a
99 simulation study to obtain additional insight into the interacting
100 physical phenomena: electromagnetics, fluid dynamics, and
101 heat transfer. The demethylation reaction in this study is
102 typically run on multitonne scale and generally employs limited
103 amounts of solvent and reagents, therewith increasing the
104 efficiency of the process and its productivity. This reaction
105 however has received little mechanistic attention, especially
106 under relevant reaction conditions. From a MW point of view,
107 the investigation of a polar reaction with high substrate/
108 product dipoles and continuously changing dielectric proper-
109 ties, as the reaction progresses, presents a great opportunity to
110 gain more knowledge and understanding of how the use of
111 MWs could potentially benefit such chemical reactions.¹⁴

112 ■ DISCUSSION

113 To assess the potential influence of different heating methods
114 on the 3MPMA to 3HPMA demethylation reaction, kinetic
115 reaction profiles (as conversion–time plots) were first

established for the case of an open vessel CTH covering the 116
90–118 °C temperature range (Figure 1A). The reaction 117 fi

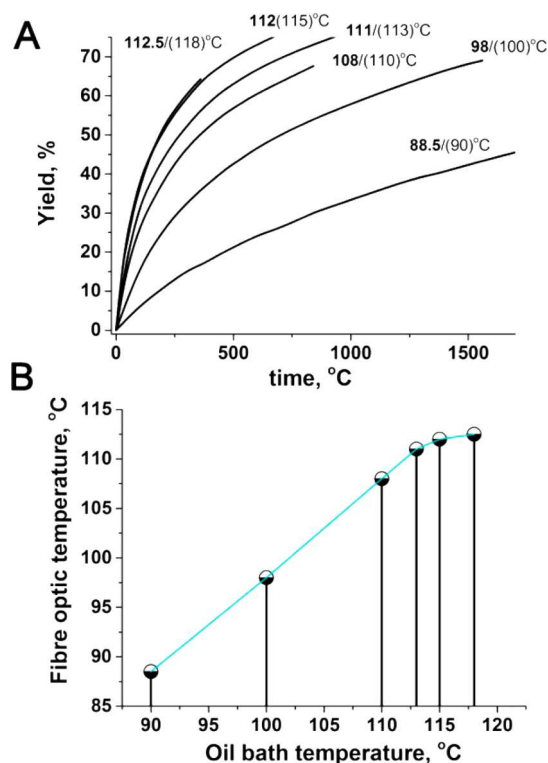


Figure 1. (A) Conversion–time plots for the CTH reaction. The temperatures displayed in bold are measured by internal fiber-optic probe while those in brackets refer to oil bath temperatures. (B) Comparison between the target (oil bath) temperatures and the temperatures recorded by internal fiber-optic probe.

118 mixture consisted of 5.038 g of 3MPMA (0.0367 mol) and
119 12.38 g of 48% HBr (0.0734 mol HBr; twice excess vis-à-vis
120 substrate), and no additional solvent was added. Temperature
121 measurement was performed in a dual way, recording both the
122 oil bath temperature and, by fiber-optic temperature probe
123 (FOTP), the internal reaction temperature. Interestingly,
124 Figure 1A shows that the rate of the reaction becomes equal
125 for oil bath temperatures ≥ 115 °C, equating by FOTP to an
126 effective internal maximal reaction temperature of 112–112.5
127 °C. A linear correlation between the target (oil bath)
128 temperatures and the recorded fiber-optic temperatures is
129 observed only up to 113 °C (oil bath) (Figure 1B).

130 Kinetic analysis of the reaction profiles in Figure 1A shows a
131 complex kinetic behavior which can generally not be explained
132 as a single first- or second-order process for the entire
133 conversion range. More specifically, the beginning and the end
134 of the reaction appear to behave as different consecutive
135 second-order processes, which interchange at the 50–60%
136 conversion level (Figure 1S). In the 90 °C case, the conversion
137 level is below 50% showing thus only the first process. To
138 explain this complex behavior, it was hypothesized that
139 throughout the reaction the number of available protons is
140 reduced by (reversible) protonation of 3HPMA (Scheme 1S).
141 This becomes particularly important in the later stages of the
142 reaction, as close to stoichiometric amounts of reagents are
143 employed in this reaction. As shown in Figure 2, this model
144 (Scheme 1S, eq 15a) fits the experimental kinetic data very well
145 for all temperatures. In a second approach, conversion–time

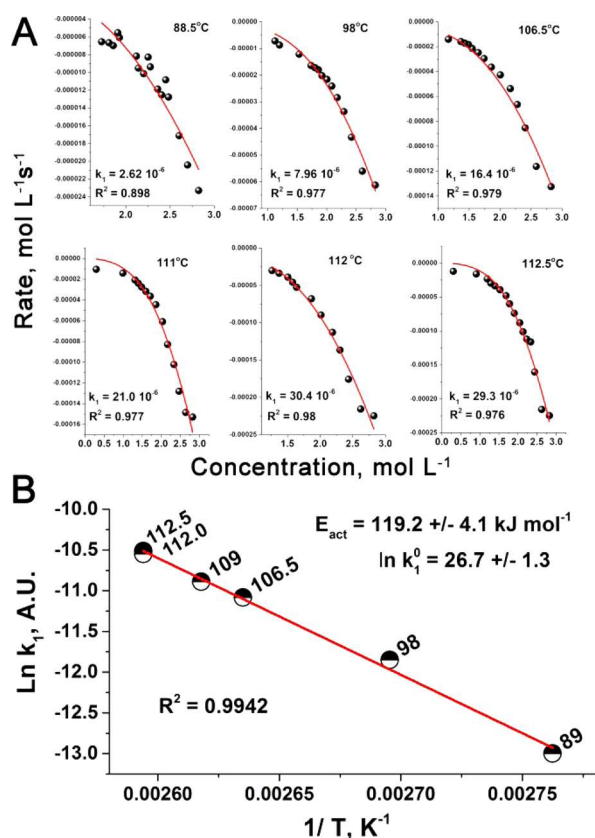


Figure 2. (A) Plots of the “reaction rate” to “substrate concentration” data for the CTH reaction and consequent fitting of the two-step model shown in Scheme 1S (eq 15a). (B) Calculated E_a and k_0 values for the CTH reaction displayed in Scheme 1S.

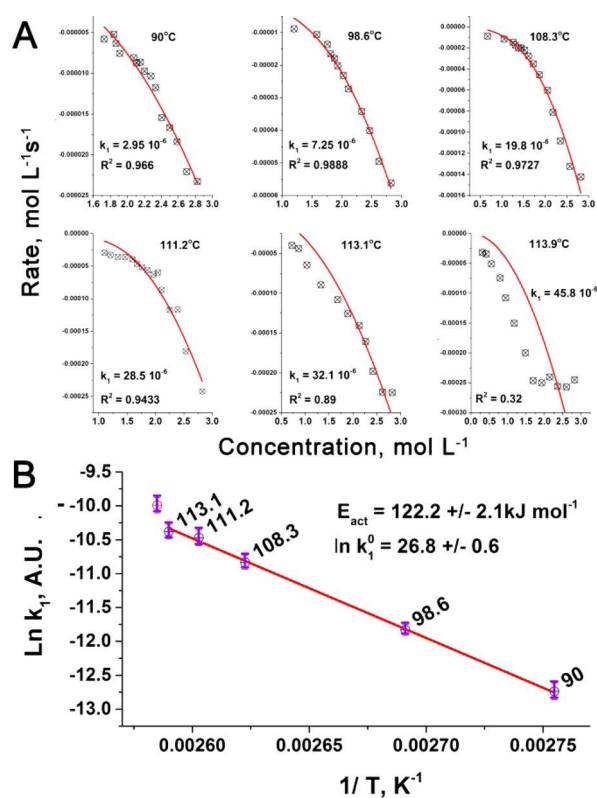


Figure 3. (A) Plots of the “reaction rate” to “substrate concentration” data for the MWH reaction and consequent fitting of the two-stage model (Scheme 1S). (B) Calculated E_a and k_0 values for the MWH reaction.

146 plots were also established for the MWH reaction. Kinetic
 147 analysis of this data shows that the two-step model presented in
 148 Scheme 1S (eq 15a) can only be applied up to 111.2 °C
 149 (FTOP) (Figure 3A). Furthermore, in the 90–113 °C range
 150 the E_a/k_0 values of the CTH and MWH reactions vary only
 151 slightly (Figures 3B/2B). As shown in Figure 4A, the reaction
 152 rate observed at ~98 °C is independent of the type of heating
 153 while at ~113 °C, MW operation leads to a markedly higher
 154 rate of reaction than observed with CTH (Figure 4B).
 155 Moreover, Figure 4B shows pronounced zero-order behavior
 156 under MW operation at 113.85 °C while under CTH, classic
 157 second-order is observed. As the recorded temperature for both
 158 heating types (MWH, CTH) is 113 °C, within experimental
 159 error, this does demonstrate a pronounced change in the
 160 reaction mechanism between the MW and the conventional
 161 thermally run reaction.

162 A multiphysics simulation, primarily using Comsol Multi-
 163 physics 5.2 (see also the section on numerical simulation in
 164 Supporting Information), was conducted to create additional
 165 insight into the electromagnetics, the fluid dynamics, and the
 166 heat transfer. To the best of our knowledge, only two studies
 167 have previously been published covering the combined
 168 simulation of electromagnetic heating and conductive/con-
 169 vective heat transfer in bench-scale MW chemistry systems.
 170 These studies both concerned heating in a CEM Discover MW
 171 device. More specifically, Robinson et al. studied the MW
 172 heating of a variety of solvents in a stirred vial, but their
 173 conducted simulation did not include a complete fluid
 174 dynamics model.¹⁵ In contrast, Sturm et al. focused on the

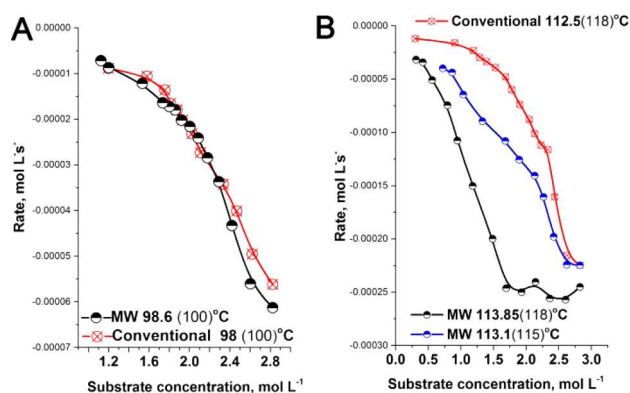


Figure 4. Illustrative overlays of the “reaction rate–substrate concentration” plots for the ConvTH and MWH reactions at 100 °C (A) and 118 °C (B).

heating of water in a MW field, including a laminar fluid
 175 dynamics model to simulate the free convection under 176
 nonstirring conditions.¹³ In addition, for the continuous flow 177
 case, Patil et al. presented an experimentally verified numerical 178
 study into a MW heated millireactor; in particular, they 179
 demonstrated temperature measurement deviations due to 180
 large thermal gradients around the sensor.¹⁶ To model the 181
 MWH demethylation reaction case adequately, a much more 182
 advanced methodology was required, covering all the relevant 183
 physical phenomena and stirring. Furthermore, to correctly 184
 predict the electromagnetic field inside the cavity and the 185
 reactor, knowledge was required of the dielectric properties of 186
 the reaction mixture at the relevant temperatures. The medium 187

188 properties were measured and determined to be $\epsilon' = 17$ and σ
 189 $= 3.3$ S/m. The dissipative (σ) term is best described as an
 190 electrical conductivity due to the high concentration of ions in
 191 solution. A visual set up is provided in Figure 5a, and additional

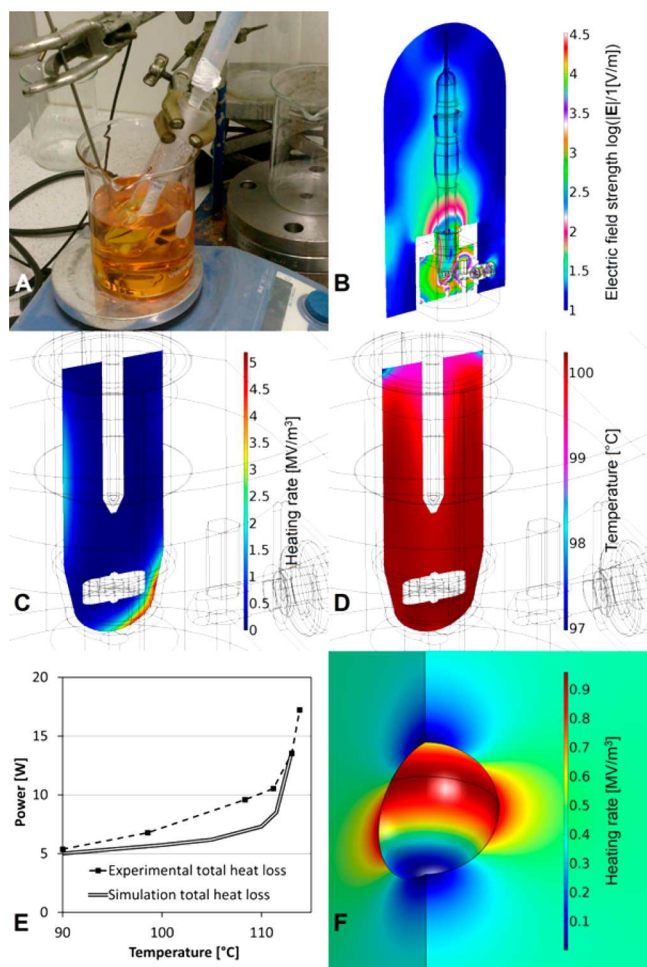


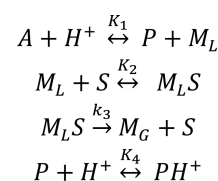
Figure 5. Simulation results of electromagnetic dissipation and heat transfer. (A) Visual setup for measurement of the dielectric properties. (B) MW field in and around the cavity applicator and reactor. (C) Heating rate distribution. (D) Temperature distribution in the reactor. (E) Overall electromagnetic dissipation in both the simulated and the experimental case versus temperature. (F) Heating rate around a bubble.

192 details are available from Supporting Information and Table 1S.
 193 The fluid agitation in the reactant mixture was simulated by
 194 applying a rotating geometrical domain, to account for stirrer
 195 bar rotation, in combination with the k - ϵ Reynolds-averaged
 196 Navier–Stokes model accounting for turbulence and turbulent
 197 heat transfer. Figure 5b–e shows the main modeling results for
 198 the multiphysics simulation. Additionally, an animated video is
 199 available from Supporting Information (video 1S). More
 200 specifically Figure 5b shows the MW field (by means of the
 201 electric field intensity on logarithmic scale) in and around the
 202 cavity applicator and reactor. The simulation shows that the
 203 electromagnetic emission and dissipation in the reactor and
 204 cavity construction materials are negligible. In addition, it also
 205 reconfirms the general nonuniformity of MW fields.¹³ The
 206 latter feature also expresses itself in the heat generation
 207 simulation presented in Figure 5c, where it can be seen that the
 208 main zone of heat generation occurs close to the MW antenna

of the cavity. However, in Figure 5d it is shown that for the
 applied stirring speed, the temperature variations in the reactor
 are too small to have any significant effect on the reaction rate,
 i.e., less than 1.5% rate variation for the highest temperatures
 and less than 0.4% below 111 °C. Figure 5e displays the overall
 electromagnetic dissipation and heat loss to the surroundings
 versus temperature for both the simulated and the experimental
 case. It can be seen that the simulation correctly approximates
 the characteristics of the experimental energy balance. The
 curves lie close to each other, and both have an accelerating
 heat loss as the temperature approaches the boiling point.
 Figure 5f shows a quasi-electrostatic analysis of the MW field
 around a bubble. The MW field is deformed by the presence of
 the bubble. Red zones, representing localized overheating, and
 blue zones, indicative of relatively cooler zones, can be
 observed. These however do not cancel out: there is a ~40%
 average increase in heat generation in a layer of ~0.1 times
 the bubble radius. Generally the evaporation of hydrobromic acid
 into a bubble extracts heat from the reactant liquid adjacent to
 this bubble due to the expansion of the bubble, which can result
 in a reduction of vapor pressure and consequently a potential
 bubble collapse. Though the flow regime in the reactor is
 turbulent due to stirring, the Kolmogorov length scale is
 calculated to be 30 to 240 μm .¹⁷ Below this scale, bubbles do
 not benefit from turbulent convective heat transfer, and their
 growth potential is limited unless a directly adjacent heat source
 is present. For the CTH case, only the bubbles contacting the
 heated reactor wall can grow, so that fewer and larger bubbles
 are formed. In comparison, for the MWH case, the presence of
 a locally enhanced volumetric heat source enables many more
 bubbles to form. This mechanism agrees well with the
 differences in boiling regime observed during experimentation;
 illustrative videos of the MWH (video 2S) and CTH (videos 3S
 and 4S) demethylation reaction at 112 °C are included in
 Supporting Information.

As the removal of MeBr gas through water/HBr vapor will be
 governed by the available surface between the reaction mixture
 and the water vapor bubbles, the occurrence of zero-order
 kinetics may relate to the available interface becoming
 insufficient to remove all produced MeBr formed at one
 given point in time. Scheme 2 represents the proposed

Scheme 2. Proposed Alternative Model for the Demethylation Reaction under MW Exposure at High Reaction Temperatures^a



^aA is 3MPMA, P is 3HPMA, M_L is methyl bromide in the liquid phase, M_G is methyl bromide in the gas phase, and S is the surface of the bubbles.

mechanism for higher temperature MW operation. The as-
 derived rate equation fits the high temperature MW kinetic data
 very well (see Scheme 2S, eq 28b, and Figure 2S). An
 additional observation in the MW transmission transient during
 experiments can be made; Figure 3S shows that fluctuations in
 the power regulation occur less rapidly with increasing reaction
 temperature, which indicates a change in medium properties as

257 the reactant mixture progresses from mechanism 1 to 2. Further
258 to the use of open vessel reactors, we also evaluated the use of a
259 closed vessel, i.e., using a pressure NMR tube for CTH and an
260 Anton Paar MW closed vessel for the MWH reaction. As
261 shown in Table 1, no distinct MW influence is observed when

Table 1. Conversion Levels for the Demethylation Reaction Performed at 118 °C in an Anton Paar MW Closed Vessel and, for the Conventional Heated Counterpart, an NMR Pressure Tube

entry	reactor type	conversion (%)		
		2 h reaction time	4 h reaction time	6 h reaction time
1	Anton Paar MW closed vessel reactor ^a	49.5	64.4	70.9
2	conventionally by NMR pressure tube ^a	47.6	64.5	70.7

^aRatio gas to liquid phase in Anton Paar reaction vessel and NMR pressure tube are the same.

262 the reaction is performed in a closed vessel reactor. Indeed, in
263 closed vessel operation no mass-transfer limitation problem
264 arises as the produced MeBr builds up a pressure of ~110 psi
265 (54.7% conversion) (Figure 4S), in that way shifting the
266 equilibrium from MeBr gas to MeBr liquid.

267 The observation of intense steam/gas bubble production in
268 the high temperature MWH reaction provided an interesting
269 opportunity for the development of a novel continuous MW
270 reactor concept in which MW energy is actually converted to
271 kinetic energy, i.e., the escaping MeBr, and the generated HBr/
272 water vapor can drive the reaction mixture around a loop. This
273 concept is similar to gas/air-lift reactors, which find common
274 application in industrial biotechnology and multiphase
275 processes, but contrary to the concept proposed here, these
276 rely on the introduction of a separate gas/air stream.¹⁸ The
277 development of a continuous MW reactor for the demethylation
278 reaction presented here holds distinct industrial advantages,
279 notably (1) a controlled release and thus manageable
280 scrubbing of toxic MeBr, (2) a continuous all-glass reactor
281 concept tailored to the use of strongly corrosive acids, avoiding
282 the need for expensive specialty alloys (e.g., Hastelloy), (3) the
283 avoidance of an expensive pumping system capable of
284 withstanding MeBr/HBr, (4) the absence of moving parts,
285 and (5) enhanced mass transfer properties. Figures 5S and 6S
286 show respectively the schematics of the circular and the
287 continuous MW reactor. A video of the circular MW reactor in
288 operation, employing a PI of 140 W, is included in Supporting
289 Information (video 5S), and the conversion–time plots are
290 shown in Figure 7S.

291 ■ CONCLUSION

292 In summary, we have shown that the main influence of MWH,
293 vis-à-vis CTH, on the kinetic parameters of an industrially
294 relevant demethylation reaction occurs only under reflux
295 conditions. Thus, the use of MWs opens a different mechanism
296 for the elimination of gaseous byproducts (e.g., MeBr), by the
297 creation of vast amounts of bubbles, therewith changing the
298 observed reaction order of the demethylation reaction from 2
299 to 0. Through modeling, the origin of this change in reaction
300 order was shown to relate to a deformation of the microwave
301 field in the presence of bubbles, leading to localized overheating
302 in the close vicinity of the bubbles. Based on these insights, a

novel continuous MW reactor concept could be proposed in 303
which MW energy is converted into kinetic energy, making the 304
production and removal of MeBr the driving force for the 305
reactor. This offers a generic reactor concept for reaction types 306
in which significant amounts of gaseous byproducts (e.g., 307
de(m)ethylation, metathesis, dehydration) are created. 308

■ ASSOCIATED CONTENT

Supporting Information

, and illustrative videos are available in the Supporting 311
Information. The Supporting Information is available free of 312
charge on the ACS Publications website at DOI: 10.1021/
jacs.7b00689. 313
314

Experimental details, additional figures, and reaction 315
schemes/models (PDF) 316

Simulation results of SAIREM TM cavity for demethylation 317
of (3-methoxyphenyl)methylammonium bromide 318
(MPG) 319

Illustrative video of the MWH demethylation reaction at 320
112 °C (MPG) 321

Illustrative video of the CTH demethylation reaction at 322
112 °C (MPG) 323

Illustrative video of the CTH demethylation reaction at 324
112 °C (MPG) 325

Video of the circular MW reactor in operation employing 326
a PI of 140 W (MPG) 327

■ AUTHOR INFORMATION

Corresponding Author

*E-mail: Duncan.Macquarrie@york.ac.uk. 329
330

ORCID

Duncan J. Macquarrie: 0000-0003-2017-7076 331
332

Notes

The authors declare no competing financial interest. 333
334

■ ACKNOWLEDGMENTS

The authors thank the European Research Council for the 336
FPVII ALTEREGO project with grant number FP7-NMP- 337
2012-309874. M.D.b. thanks Ms. A. Storey for the specialty 338
glassware and Mr. C. Mortimer for consultation on practical 339
reactor development. G.S.J.S. acknowledges Dr. J. W. R. Peeters 340
for valuable feedback on the turbulence modeling, as well as the 341
support staff of COMSOL B.V. (Zoetermeer, NL) for their 342
prompt technical support. 343

■ REFERENCES

- (1) Wathey, B.; Tierney, J.; Lidstrom, P.; Westman, J. *Drug Discovery Today* **2002**, *7*, 373–380. 345
346
- (2) Kappe, C. O.; Pieber, B.; Dallinger, D. *Angew. Chem., Int. Ed.* **2013**, *52*, 1088–1094. 347
348
- (3) de la Hoz, A.; Diaz-Ortiz, A.; Moreno, A. *Chem. Soc. Rev.* **2005**, *34*, 164–178. 349
350
- (4) Kappe, C. O. *Angew. Chem., Int. Ed.* **2013**, *52*, 7924–7928. 351
- (5) Dudley, G. B.; Richert, R.; Stiegman, A. E. *Chem. Sci.* **2015**, *6*, 2144–2152. 352
353
- (6) Wu, Y.; Gagnier, J.; Dudley, G. B.; Stiegman, A. E. *Chem. Commun.* **2016**, *52*, 11281–11283. 354
355
- (7) Kappe, C. O. *Acc. Chem. Res.* **2013**, *46*, 1579–1587. 356
- (8) Ashley, B.; Lovingood, D. D.; Chiu, Y.-C.; Gao, H.; Owens, J.; Strouse, G. F. *Phys. Chem. Chem. Phys.* **2015**, *17*, 27317–27327. 357
358
- (9) Fan, J. J.; De Bruyn, M.; Budarin, V. L.; Gronnow, M. J.; Shuttleworth, P. S.; Breeden, S.; Macquarrie, D. J.; Clark, J. H. *J. Am. Chem. Soc.* **2013**, *135*, 11728–11731. 359
360
361

- 362 (10) Breckenridge, R. J.; Nicholson, S. H.; Nicol, A. J.; Suckling, C. J.;
363 Leigh, B.; Iversen, L. *J. Neurochem.* **1981**, *37*, 837–844.
- 364 (11) Travnicek, Z.; Sipl, M.; Popa, I. *J. Coord. Chem.* **2005**, *58*, 1513–
365 1521.
- 366 (12) Christiaens, S.; Vantghem, X.; Radoiu, M.; Vanden Eynde, J. J.
367 *Molecules* **2014**, *19*, 9986–9998.
- 368 (13) Sturm, G. S. J.; Verweij, M. D.; van Gerven, T.; Stankiewicz, A.
369 I.; Stefanidis, G. D. *Int. J. Heat Mass Transfer* **2012**, *55*, 3800–3811.
- 370 (14) Waghmode, S. B.; Mahale, G.; Patil, V. P.; Renalson, K.; Singh,
371 D. *Synth. Commun.* **2013**, *43*, 3272–3280.
- 372 (15) Robinson, J.; Kingman, S.; Irvine, D.; Licence, P.; Smith, A.;
373 Dimitrakis, G.; Obermayer, D.; Kappe, C. O. *Phys. Chem. Chem. Phys.*
374 **2010**, *12*, 4750–4758.
- 375 (16) Patil, N. G.; Benaskar, F.; Meuldijk, J.; Hulshof, L. A.; Hessel,
376 V.; Schouten, J. C.; Esveld, E. D. C.; Rebrov, E. V. *AIChE J.* **2014**, *60*,
377 3824–3832.
- 378 (17) Pope, S. B. *Turbulent flows*; Cambridge University Press:
379 Cambridge, 2000.
- 380 (18) Drandev, S.; Penev, K. I.; Karamanev, D. *Chem. Eng. Sci.* **2016**,
381 *146*, 180–188.